Aging in binary-state models: The Threshold model for complex contagion

David Abella●,[*] Maxi San Miguel●, and José J. Ramasco●
Instituto de Física Interdisciplinar y Sistemas Complejos IFISC (CSIC-UIB),
Campus Universitat Illes Balears, 07122 Palma de Mallorca, Spain

We study the non-Markovian effects associated with aging for binary-state dynamics in complex networks. Aging is considered as the property of the agents to be less prone to change their state the longer they have been in the current state, which gives rise to heterogeneous activity patterns. In particular, we analyze aging in the Threshold model, which has been proposed to explain the process of adoption of new technologies. Our analytical approximations give a good description of extensive Monte Carlo simulations in Erdős-Rényi, random-regular and Barabási-Albert networks. While aging does not modify the cascade condition, it slows down the cascade dynamics towards the full-adoption state: the exponential increase of adopters in time from the original model is replaced by a stretched exponential or power law, depending on the aging mechanism. Under several approximations, we give analytical expressions for the cascade condition and for the exponents of the adopters' density growth laws. Beyond random networks, we also describe by Monte Carlo simulations the effects of aging for the Threshold model in a two-dimensional lattice.

I. INTRODUCTION

Stochastic binary-state models are a versatile tool to describe a variety of natural and social phenomena in systems formed by many interacting agents. Each agent is considered to be in one of two possible states: susceptible or infected, adopters or nonadopters, democrat or republican, etc., depending on the context of the model. The interaction among agents is determined by the underlying network and the dynamical rules of the model. There are many examples of binary-state models, including processes of opinion formation [1–4], disease or social contagion [5,6], etc. Extended and modified versions of these models can lead to very different dynamical behaviors than in the original model. As examples, the use of multilayer [7–9] or time-dependent networks [10], higher-order interactions [11–13], nonlinear collective phenomena [14,15], noise [16], and non-Markovian [17–20] effects induce significant changes to the dynamics.

A well-known binary-state model is the Threshold model [21], introduced by Granovetter [5], for rumor propagation, adoption of new technologies, riots, stock market herds, political and environmental campaigns, etc. These are examples of *complex contagion* processes [22,23] in which contagion, at variance with *simple contagion* (such as in the voter and SIS models), requires simultaneous exposure to multiple adopter neighbors and a threshold fraction of neighboring agents

that have already undergone contagion. Complex contagion implies a process of group or many-agent interactions built from a combination of pairwise interactions. The discontinuous phase transition and the cascade condition exhibited by the Threshold model were predicted with analytical tools in Ref. [21]. This model has been extensively studied in regular lattices and small-world networks [22], random graphs [24], modular and community structure [25], clustered networks [26,27], hypergraphs [11], homophilic networks [28], etc. Moreover, recent studies also include variants of the adoption rules, including the impact of opinion leaders [29] and seed size [30], on-off threshold [31], and the competition between simple and complex contagion [28,32,33]. Additionally, the Threshold model has been confronted with several sources of empirical data [34–41].

Theoretical and computational studies of stochastic binary-state models, including the Threshold model, usually rely on a Markovian assumption for its dynamics. However, there is strong empirical evidence against this assumption in human interactions. For example, bursty non-Markovian dynamics with heavy-tail inter-event time distributions, reflecting temporal activity patterns, have been reported in many studies [42–47]. The understanding of these non-Markovian effects is in general a topic of current interest [17–19,48]. In particular, for the Threshold model, memory effects have been included as past exposures' memory [49], message-passing algorithms [50], memory distributions for retweeting algorithms [51], and timers [52].

Aging is an important non-Markovian effect that we address in this paper for binary-state models. Aging accounts for the influence that the persistence time of an agent in a given state modifies the transition rate to a different state [20,53–56], so that the longer an agent remains in a given state, the smaller is the probability to change it. Aging effects have

---

[*]david@ifisc.uib-csic.es

already been shown to modify binary-state dynamics very significantly. For example, aging is able to produce coarsening towards a consensus state in the voter model [48,54], to induce continuous phase transitions in the noisy voter model [19,57], or to modify the phase diagram and nonequilibrium dynamics of the Schelling segregation model [58].

In the specific context of innovation adoption, other mechanisms of inertia or resistance to adopt the technology have already been introduced. In fact, the original approach of Rogers [59] considers a fraction of "laggards" that will resist innovating until a large majority of the population has already adopted it. Similar articles highlight the importance of timing interactions [60] and the effect of "contrarians" (tendency to act against the majority), which has an important impact on the dynamics [61,62]. In Ref. [62], it is discussed how different technologies may show different adoption cascades regarding the balance between advertisement and resistance to change.

In this paper, we provide a general theoretical framework to discuss aging effects building upon a general Markovian approach for binary-state models [63,64]. We build a general master equation for any binary-state model with temporal activity patterns and we propose two different aging mechanisms giving rise to heterogeneous activity patterns, characterized by flat-tail inter-event time distributions. As an example, we apply this framework to the Threshold model for complex contagion. Theoretical predictions are matched with extensive Monte Carlo simulations in different networks. In addition, the role of both aging mechanisms is also studied in a two-dimensional Moore lattice.

The paper is organized as follows. In the next section, we describe the original Threshold model and introduce exogenous and endogenous aging in the model. In Sec. III, numerical results are reported and contrasted with theoretical predictions for different complex networks. For completeness, in Sec. IV, the case of a two-dimensional (2D) lattice is analyzed. The final section contains a summary and a discussion of the results. The derivation of the approximate master equation (AME) for general binary-state dynamics with aging effects is given in the Appendix.

II. AGING AND THE THRESHOLD MODEL

In the standard Threshold model [5,21], one considers a network of N interacting agents. Each node of the network represents an agent i with a binary-state variable $\sigma_i = \{0, 1\}$ and a given threshold T ($0 < T < 1$). The state indicates whether or not the agent has adopted a technology (or joined a riot, spread a meme or fake news, etc.). We use the wording of a technology adoption process for the rest of the paper. If a node i (with k neighbors) has not adopted ($\sigma_i = 0$) the technology, it becomes an adopter ($\sigma_i = 1$) if the fraction m/k of the neighbors' adopters exceeds the threshold T. Adopter nodes cannot go back to the nonadopter state.

In the Threshold model with aging, each agent has an internal time $j = 0, 1, 2, \ldots$ (in Monte Carlo units) as in Refs. [19,20,48,53–55,57,58,65]. As an initial condition, we set $j = 0$ for all nodes. In Monte Carlo simulations, we follow a random asynchronous update in which agents are activated in discrete time steps with probability $p_A(j) = 1/(j + 2)$.

When a nonadopter agent is activated, he or she changes state according to the threshold condition $m/k > T$. We will consider two different aging mechanisms, endogenous and exogenous aging [54], which account for the power-law inter-event time distributions empirically observed in human interactions [46]. For endogenous aging, the internal time measures the time spent in the current state: If an agent in an updating attempt is not activated or does not adopt, the internal time increases by one unit. Therefore, the longer an agent has remained without adopting the technology, the more difficult it is for him or her to adopt it.

For exogenous aging, the internal time accounts for the time since the last attempt to change state: In each updating attempt in which the agent is activated, the internal clock resets to $j = 0$ even if there is no adoption. In this case, aging is understood as a resistance to adopt the technology the longer the agent has not been induced to consider adoption by some external influence.

III. DYNAMICS ON COMPLEX NETWORKS

In this section, we discuss the Threshold model with endogenous and exogenous aging in three different complex networks: random regular [66], Erdős-Rényi [67], and Barabási-Albert [68].

A. Numerical results

For the considered networks, the Threshold model undergoes a discontinuous phase transition at a certain critical value T_c, which is called the cascade condition [21]. For $T < T_c$, a small initial seed of adopters triggers a global cascade where, on average, a significant proportion of agents in the system adopts the technology (change from $\sigma_i = 0$ to 1). In our analysis, the initial condition is set to favor cascades: one agent i with degree $k_i = z$ is selected randomly and all his or her neighbors are initially adopters, as in Refs. [22,30]. For $T > T_c$, there are few cascade occurrences and none of them are global. The cascade condition dependence with the average degree z of the underlying network has been studied in Refs. [21,24]. For the two aging mechanisms considered here, Monte Carlo simulations in random graphs show that the T_c dependence on z is very similar to the one for the model without aging (see Fig. 1). Therefore, for large connected networks, it tends to the same cascade condition derived for the original Threshold model (which for Erdős-Rényi (ER) graphs is $T_c = 1/z$ [21]). This result is not obvious *a priori* because aging has been shown to modify the final state in several models [19,20,48,53–55,57,58,65]. This is discussed in detail in Appendix A.

Even though aging in the Threshold model does not modify the cascade condition, it has a large impact in the complex contagion cascade dynamics (Fig. 2). From Monte Carlo simulations in a random regular graph, we find that without aging, the average fraction of adopters follows an initial exponential increase with time [see Figs. 2(a) and 3(a)],

$$\rho(t) \sim \rho_0 \, e^{\alpha t}, \tag{1}$$

where ρ_0 is the initial fraction of adopters (seed). This behavior is universal for all values of the control parameters z
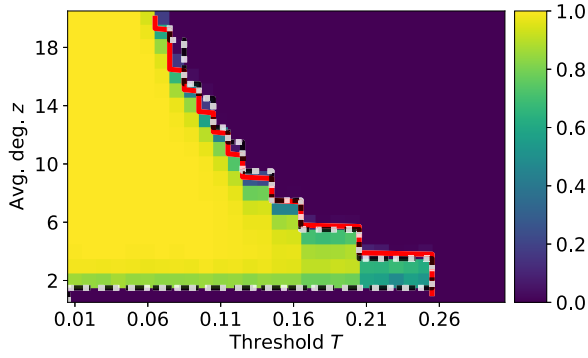
FIG. 1. Average density ρ of adopters for an Erdős-Rényi graph of mean degree z using a model with threshold T. Color-coded values of ρ are from Monte Carlo simulations of the model without aging in a graph with $N = 10\,000$ agents. Black dashed and white dotted lines correspond to the T_c value obtained numerically for the model with exogenous and endogenous aging, respectively. Monte Carlo simulations are averaged over $M = 5 \times 10^4$ realizations. The red solid line is the analytical approximation of the cascade boundary, from Eq. (17), which is the same with and without aging.

and T below the cascade condition. In addition, we investigated the approach to the full-adopt state ($\rho = 1$) and we found that the number of nonadopters follows an exponential decay $1 - \rho(t) \sim e^{-t}$ for all values of the control parameters [see inset in Fig. 3(a)].

When aging is introduced, the cascade dynamics are much slower than an exponential law [see Fig. 2(b)]. For endogenous aging, all agents that are nonadopters have the same activation probability $p_A(j)$, which decreases at each time step. This gives rise to cascade dynamics that are well fitted
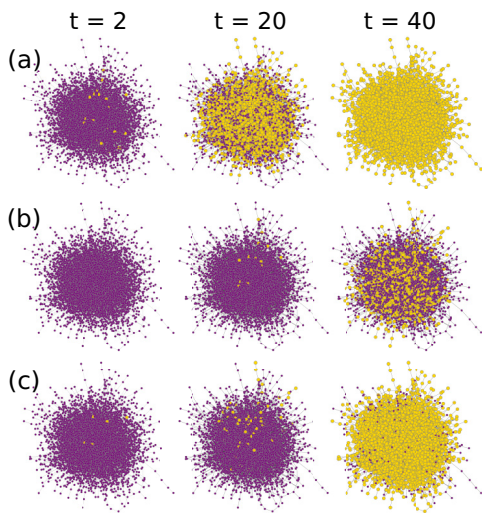

FIG. 2. Cascade spreading for (a) the original Threshold model, and the versions with (b) endogenous and (c) exogenous aging. Yellow nodes are adopters and purple nodes are nonadopters. Time increases from left to right. Monte Carlo simulations are performed in an Erdős-Rényi network with mean degree $z = 3$ and $T = 0.22$. System size is $N = 8\,000$.
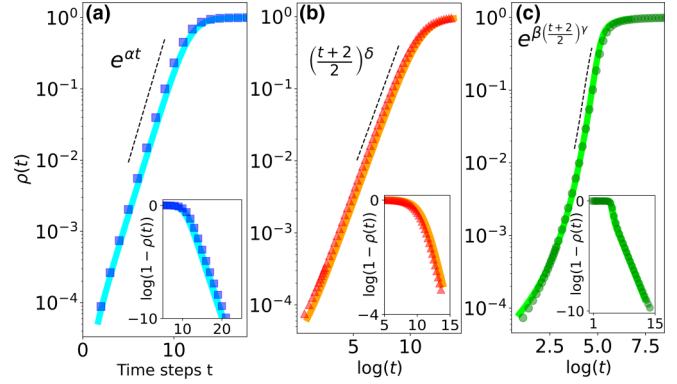

FIG. 3. Cascade dynamics and fall to the full-adopt state ($\rho \sim 1$) of the Threshold model (a) without aging, and the versions with (b) endogenous and (c) exogenous aging effects. At (b) and (c), the evolution is plotted as a function of the logarithm of time, $\ln (t)$, in Monte Carlo steps, as in the insets. The underlying network is a 3-regular random graph and the threshold is $T = 0.2$. The exponent values are $\alpha \simeq 1.0$, $\beta \simeq 1.14$, $\gamma \simeq 0.38$, and $\delta \simeq 1.0$. Numerically integrated solutions of Eq. (4) (solid lines) accurately describe the numerical results. Monte Carlo simulations are averaged over $M = 5 \times 10^4$ realizations in a network of $N = 1.6 \times 10^5$ nodes.

by a power-law increase [see Fig. 3(b)],

$$\rho(t) \sim \rho_0 \left(\frac{t+2}{2} \right)^\delta. \tag{2}$$

For exogenous aging, we observe a slow adoption spread at the beginning followed by a cascade where almost all agents adopt the technology [Fig. 2(c)]. This behavior is well fitted with a stretched exponential increase of the number of adopters [see Fig. 3(c)],

$$\rho(t) \sim \rho_0 \, e^{\beta \, ((t+2)/2)^\gamma}. \tag{3}$$

For both aging mechanisms, in the last stages of evolution, a few "stubborn" nonadopters remain, although the environment favors the adoption. Due to the chosen activation probability, the number of nonadopters decay with a power law $1 - \rho(t) \sim 1/(t+2)$ in both cases [see insets of Figs. 3(b) and 3(c)].

Comparing the evolution of the original model with one of the versions with aging, we observe an important separation of timescales. While for the original model, the time to reach the steady state follows a logarithmic increase with the system size, the versions with endogenous and exogenous aging show a power law and a power-logarithmic dependence, respectively (see Fig. 4). Therefore, the timescale separation between the original model and the versions with aging increases as we increase the system size, and thus the aging effects are more relevant for large systems.

The power law and the stretched exponential dynamics for endogenous and exogenous aging, respectively, are observed for all parameter values z and T below the cascade condition ($T < T_c$) and for all system sizes. This is shown in Fig. 5 for random-regular, Erdős-Rényi, and Barabási-Albert networks. In particular, we show that the time-dependent behavior for different system sizes collapses to a single curve when time is scaled with the system size-dependent timescale (previously
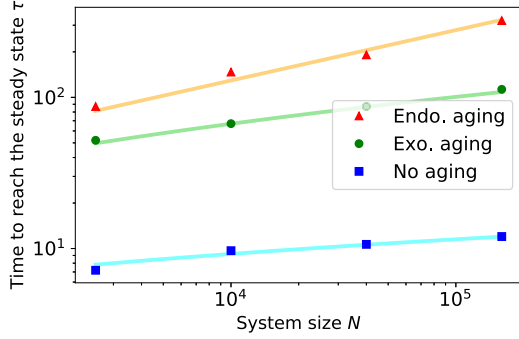
FIG. 4. Average time to reach the steady state ($\rho > 0.9$) τ as a function of the system size N for the original Threshold model and the versions with endogenous and exogenous aging. The underlying network is a 5-regular random graph and the threshold is $T = 0.12$. Monte Carlo simulations are averaged over $M = 5 \times 10^4$ realizations. Solid lines are the system size-dependent timescale: For the original model, $\tau_{\text{NO AG}} = (1/\alpha)\ln(N)$, and for the endogenous ($\tau_{\text{ENDO}} = 2N^{1/\delta} - 2$) and exogenous ($\tau_{\text{EXO}} = 2[\ln(N)/\beta]^{1/\gamma} - 2$) aging, which follows from the dynamics from Eqs. (1)–(3). The exponents α, β, γ, and δ are fitted exponents.

analyzed in Fig. 4) that follows from either the power-law dynamics ($\tau_{\text{ENDO}} = 2N^{1/\delta} - 2$) or the stretched exponential law ($\tau_{\text{EXO}} = 2[\ln(N)/\beta]^{1/\gamma} - 2$). Notice that the scaling of the y axis is necessary for Figs. 5(d)–5(f) to show a linear dependence (for all system sizes) due to the stretched exponential increase.

A different question is the dependence of the exponents of the power law and stretched exponential with the parameters z and T. Numerical results from fitted Monte Carlo simulations for $\alpha(z, T)$, $\delta(z, T)$, and $\gamma(z, T)$ are shown in Figs. 6 and 7. For a random-regular graph, as apparent from Fig. 5, the exponents do not depend on the parameter T up to T_c [so the exponents are dependent only on z, $\alpha(z)$, $\gamma(z)$, and $\delta(z)$], while for Erdős-Rényi and Barabási-Albert networks, the value of the exponents decreases with T when approaching T_c, indicating a slowing down of the dynamics. Also, for these two latter networks, the exponents present a maximum value at a certain value of z. This maximum value at a certain z for a fixed T can be understood as being between the two critical lines of Fig. 1.

B. General mathematical description

To account for the non-Markovian dynamics introduced by the aging mechanism, we need to go beyond the standard mathematical descriptions of the Threshold model [24,25,64]. We do so using a Markovian description by enlarging the number of variables [19,48]. Namely, we classify the agents with degree k, number of adopter neighbors, m, and age j as different sets in a compartmental model in a general framework for binary-state dynamics in complex networks [21,63,64]. Assuming a local treelike network structure, such as the one generated using the configuration model for a generic degree distribution p_k [69,70] or Erdős-Rényi model, we derive a general master equation [71] for binary-state dynamics with temporal activity patterns in complex net-

works considering the following possible transitions (see Appendix B for details):

(i) A susceptible [infected] node changes state and resets internal age with probability $F(k, m, j)$ [$R(k, m, j)$].

(ii) A susceptible [infected] node remains in the same state and resets internal age to zero ($j \to 0$) with probability $F_R(k, m, j)$ [$R_R(k, m, j)$].

(iii) A susceptible [infected] node remains in the same state and ages ($j \to j + 1$) with probability $F_A(k, m, j)$ [$R_A(k, m, j)$].

See a schematic representation in Fig. 11. Note that here we introduce epidemics notation of susceptible or infected nodes [63,64], but it is immediately translated to the non-adopter or adopter situation of our model. For the specific case of the Threshold model, the dynamics are monotonic and $R(k, m, j) = 0$ (no adopter becomes a nonadopter). Moreover, when an agent becomes an adopter, there are neither resetting nor aging events, $R_R(k, m, j) = R_A(k, m, j) = 0$. This means as well that equations for the nonadopter $s_{k,m,j}$ and adopter $i_{k,m,j}$ nodes are independent. Thus, we can write the following rate equations for the evolution of the fraction $s_{k,m,j}(t)$ of k-degree nonadopter nodes with m infected neighbors and age j:

$$
\begin{aligned}
\frac{ds_{k,m,j}}{dt} = {} & -s_{k,m,j} - (k-m)\beta^s s_{k,m,j} \\
& + (k-m+1)\beta^s s_{k,m-1,j-1} \\
& + F_A(k, m, j-1) s_{k,m,j-1},
\end{aligned}
$$

$$
\begin{aligned}
\frac{ds_{k,m,0}}{dt} = {} & -s_{k,m,0} - (k-m)\beta^s s_{k,m,0} \\
& + \sum_{l=0} F_R(k, m, l) s_{k,m,l},
\end{aligned} \tag{4}
$$

where β^s is a nonlinear function of $s_{k',m',j'}$ for all values of k', m', and j' [see Eq. (B4)]. The remaining step is to explicitly define the transition probabilities for our aging mechanisms. For both exogenous and endogenous aging, the adoption probability is the probability that an agent is activated and has a fraction of adopters that exceeds the threshold T, which means that

$$
F(k, m, j) = p_A(j)\,\theta(m/k - T), \tag{5}
$$

where $\theta(\cdot)$ is the Heaviside step function.

The reset and aging probabilities for endogenous and exogenous aging mechanisms are different. The simplest case is endogenous aging, where there is no reset $F_R(k, m, j) = 0$ and agents increase, by one, the age with probability

$$
F_A(k, m, j) = 1 - F(k, m, j) = 1 - p_A(j)\,\theta(m/k - T). \tag{6}
$$

When aging is exogenous, the reset probability is the probability to activate and not adopt,

$$
F_R(k, m, j) = p_A(j)\,[1 - \theta(m/k - T)]. \tag{7}
$$

Thus, agents that age are just the ones that do not activate, $F_A(k, m, j) = 1 - p_A(j)$.

Using these definitions, we have integrated Eq. (4) numerically for the Threshold model with both endogenous
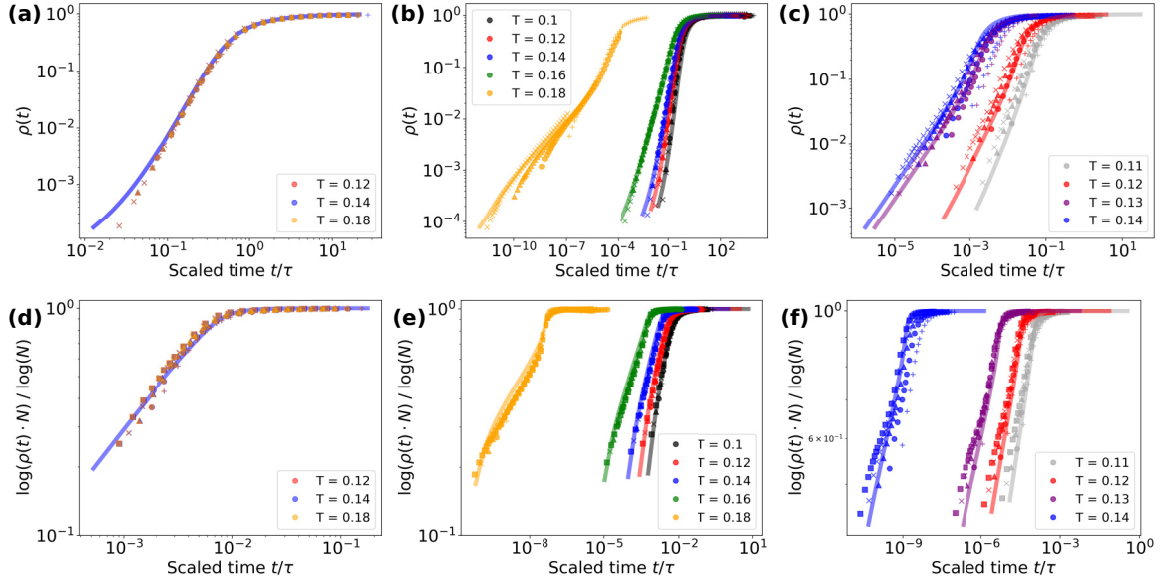
FIG. 5. Cascade dynamics of the Threshold model with (a)–(c) endogenous and (d)–(f) exogenous aging. From the left column to the right: (a), (d) a random regular graph with degree $z = 5$, (b), (e) an Erdős-Rényi graph with average degree $z = 5$, and (c), (f) a Barabási-Albert graph with average degree $z = 8$. Different colors indicate different values of T and markers correspond to different system sizes: $N = 2\,500$ (plus), $10\,000$ (circles), $40\,000$ (triangles), $160\,000$ (crosses), and $640\,000$ (squares). Time is scaled according to the system size for each model: $\tau_{\text{EXO}} = 2[\ln(N)/\beta]^{1/\gamma} - 2$, $\tau_{\text{ENDO}} = 2N^{1/\delta} - 2$, where β, γ, and δ are the fitted exponents from the behavior according to Eqs. (2) and (3). Solid lines are obtained from the solutions of Eq. (13). Monte Carlo simulations are averaged over $M = 5 \times 10^4$ realizations.

and exogenous aging. Numerical solutions give good agreement with Monte Carlo simulations (see Fig. 3). However, in a general network, considering a cutoff for the degree $k = 0, \ldots, k_{\max}$ and age $j = 0, \ldots, j_{\max}$, the number of differential equations to solve is $(k_{\max} + 1)(k_{\max} + 1)(j_{\max} + 1)$ according to the three subindexes of the variable $s_{k,m,j}$. This number grows with the largest degree square and largest age considered and, thus, some further approximations are needed to obtain a convenient reduced system of differential equations.

As an ansatz, we assume that timing interactions can be effectively decoupled from the adoption process so the solution of Eq. (4) can be written as

$$s_{k,m,j}(t) = s_{k,m}(t)\, G_j(t), \tag{8}$$

where $s_{k,m}$ is the fraction of nonadopters with degree k and m infected neighbors, $s_{k,m} = \sum_j s_{k,m,j}$, and there is an age distribution $G_j(t)$, independent of the adoption process.

If we sum over the variable age j in Eq. (4), we can rewrite the following rate equations for the variables $s_{k,m}$:

$$\frac{ds_{k,m}}{dt} = -\langle p_A\rangle\, \theta(m - kT)\, s_{k,m} - (k - m)\, \beta^s\, s_{k,m}$$
$$+ (k - m + 1)\, \beta^s\, s_{k,m-1}, \tag{9}$$

where aging effects are just included in $\langle p_A\rangle(t)$,

$$\langle p_A\rangle(t) = \sum_{j=0}^{\infty} p_A(j)\, G_j(t). \tag{10}$$

Using the definition of the fraction of k-degree agents adopters $\rho_k(t)$,

$$\rho_k(t) = 1 - \sum_{j=0}^{\infty} \sum_{m=0}^{k} s_{k,m,j}, \tag{11}$$

and along the lines of Ref. [64], we use the exact solution

$$s_{k,m} = [1 - \rho_k(0)]\, B_{k,m}[\phi], \tag{12}$$

where $B_{k,m}[\phi]$ is the binomial distribution with k attempts, m successes, and with success probability ϕ. From this point, we derive from Eq. (9) a reduced system of two coupled differential equations for the fraction of adopters, $\rho(t) = \sum_k p_k \rho_k(t)$, and an auxiliary variable $\phi(t)$ (see details in Ref. [64]):

$$\frac{d\rho}{dt} = \langle p_A\rangle[h(\phi) - \rho],$$
$$\frac{d\phi}{dt} = \langle p_A\rangle[g(\phi) - \phi], \tag{13}$$

where $\phi(t)$ can be understood as the probability that a randomly chosen neighbor of a nonadopter node is an adopter at time t. The functions $h(\phi)$ and $g(\phi)$ are nonlinear functions of this variable ϕ,

$$h(\phi) = \sum_{k=0}^{\infty} p_k \left\{ \rho_k(0) + [1 - \rho_k(0)] \sum_{m=kT}^{k} B_{k,m}[\phi] \right\},$$
$$g(\phi) = \sum_{k=0}^{\infty} \frac{k}{z} p_k \left\{ \rho_k(0) + [1 - \rho_k(0)] \sum_{m=kT}^{k} B_{k-1,m}[\phi] \right\}. \tag{14}$$

When $\langle p_A\rangle$ is replaced by a constant, Eqs. (13) reduce to previous results for the original model [25].

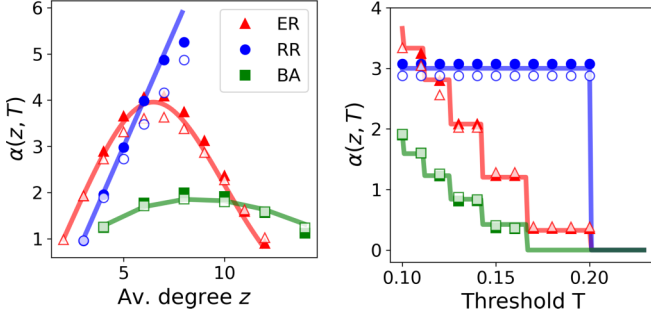FIG. 6. Exponent α for the original Threshold model (empty markers) and δ for the version with endogenous aging (filled markers) for different values of the average degree z (and $T = 0.1$) (left) and as a function of T for fixed z (right). Different markers indicate results from Monte Carlo simulations with different topologies: red triangles indicate an Erdős-Rényi (ER) graph, blue circles indicate a random-regular (RR) graph, and green squares indicate a Barabási-Albert (BA) graph. In the right panel, the average degree is fixed $z = 5$ for ER and RR, and $z = 8$ for the BA. Predicted values by Eq. (22) (solid lines) fit the results for each topology. System size is fixed at $N = 4 \times 10^6$ for the original model and $N = 3.2 \times 10^5$ for the version with aging.

Determining the distribution $G_j(t)$ is not easy. For endogenous aging, all nonadopters have the same age at each time step and $G_j(t) = \delta(j - t)$ [where $\delta(\cdot)$ is the Dirac delta function]. Therefore, $\langle p_A \rangle = 1/(t + 2)$. The numerical solution of Eq. (13) gives a good agreement with Monte Carlo simulations [see Figs. 5(a)–5(c)]. For the case of exogenous aging, the reset of the internal clock makes more difficult a choice for $G_j(t)$. Inspired by the stretched exponential behavior of $\rho(t)$ observed from Monte Carlo simulations, we propose $\langle p_A \rangle = 1/(t + 2)^\mu$. For $\mu = 0.75$, the numerical solutions of Eq. (13) gives a very good agreement with our Monte Carlo simulations [see Figs. 5(d)–5(f)].
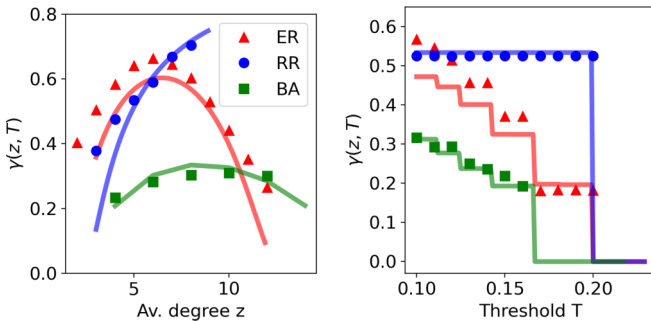

FIG. 7. Exponent γ for the Threshold model with exogenous aging for different values of the average degree z ($T = 0.1$) (left) and as a function of T for fixed z (right). Different markers indicate results from Monte Carlo simulations with different topology: red triangles indicate an Erdős-Rényi (ER) graph, blue circles indicate a random-regular (RR) graph, and green squares indicate a Barabási-Albert (BA) graph. In the right panel, the average degree is fixed $z = 5$ for ER and RR, and $z = 8$ for the BA. Predicted values by numerical integration of Eqs. (13) (solid lines) fit approximately the results for each topology. System size is fixed at $N = 3.2 \times 10^5$.

C. Analytical results

To obtain an analytical result for the cascade condition and for the exponents of the predicted exponential, stretched-exponential, and power-law cascade dynamics that we fitted from Monte Carlo simulations, we need to go a step beyond the numerical solution of our approximated differential equations [Eqs. (4) and (13)].

For a global cascade to occur, it is necessary that the variable $\phi(t)$ grows with time. If we assume a small initial seed [$\rho_k(0) \to 0$], Eq. (13) can be rewritten as in Ref. [24],

$$\frac{d\phi}{dt} = \langle p_A \rangle \left(-\phi + \sum_{k=1}^{\infty} \frac{k}{z} p_k \sum_{m=kT}^{k} B_{k-1,m}[\phi] \right). \quad (15)$$

Rewriting the sum term as $\sum_{l=0}^{\infty} C_l \phi^l$, with coefficients

$$C_l = \sum_{k=l}^{\infty} \sum_{m=0}^{l} \binom{k-1}{l} \binom{l}{m} (-1)^{l+m} \frac{k}{z} p_k \theta(m/k - T), \quad (16)$$

we linearize Eq. (15) around $\phi = 0$,

$$\frac{d\phi}{dt} \approx \langle p_A \rangle (C_1 - 1) \phi. \quad (17)$$

The solution for Eq. (17) is then

$$\phi(t) = \rho_0 e^{(C_1 - 1) \int_0^t \langle p_A \rangle (s) \, ds}, \quad (18)$$

given that $\phi(0) = \rho_0$.

Since $\langle p_A \rangle(t)$ is always positive, global cascades occur when $(C_1 - 1) > 0$. This cascade condition does not depend on the aging term $\langle p_A \rangle(t)$, and thus it is the same as for the Threshold model without aging. In Fig. 1, the red solid line is the result of this analytical calculation and it is in good agreement with the numerical results.

Linearization is also useful to determine the time dependence of the cascade process. Assuming a small initial seed and rewriting the term $h(\phi)$ as $\sum_{l=0}^{\infty} K_l \phi^l$, the linearized equation for the fraction of adopters $\rho(t)$ becomes

$$\frac{d\rho}{dt} \approx \langle p_A \rangle (K_1 - 1) \phi, \quad (19)$$

where the coefficients K_l are

$$K_l = \sum_{k=l}^{\infty} \sum_{m=0}^{l} \binom{k}{l} \binom{l}{m} (-1)^{l+m} p_k \theta(m/k - T). \quad (20)$$

A solution for the fraction of adopters $\rho(t)$ can be obtained from Eqs. (18) and (19). For the case of the Threshold model without aging, setting $\langle p_A \rangle = 1$, the solution is an exponential cascade dynamics,

$$\rho(t) = \rho_0 e^{(C_1 - 1) t}. \quad (21)$$

Therefore, the number of adopters, $\rho(t)$, follows an exponential increase with exponent $\alpha(z, T)$,

$$\alpha(z, T) = C_1 - 1 = \sum_{k=0}^{\lfloor 1/T \rfloor} \frac{k(k-1)}{z} p_k - 1, \quad (22)$$

where C_1 is computed from Eq. (16).

For endogenous aging, the same derivation is valid to determine the exponents $\delta(z, T)$. Using $\langle p_A \rangle = 1/(t + 2)$, the

fraction of adopters follows a power-law dependence,

$$\rho(t) = \rho_0 \left(\frac{t+2}{2} \right)^{(C_1-1)}. \tag{23}$$

The exponent reported for the power-law cascade dynamics $\delta(z, T)$ turns out to be, therefore, the same exponent as the one for the exponential behavior where there is no aging: $\delta(z, T) = \alpha(z, T) = C_1 - 1$. Figure 6 compares the prediction of Eq. (22) with the results computed from Monte Carlo simulations. There is a good agreement for both the Barabási-Albert and Erdős-Rényi networks for all values of T and z. For a random-regular graph, the predicted dependence, $\alpha(z) = z - 2$, is not a good approximation for large z. This is because the presence of small cycles increases importantly in a random-regular graph as the average degree z grows [72] and the locally tree assumption made for the derivation of the rate equations [Eq. (4)] is no longer valid. A different approach is necessary for clustered networks (as in Ref. [73] for the Threshold model).

For exogenous aging, an analytical expression for the exponent $\gamma(z, T)$ is not obtained following this methodology. Still, we can fit the exponent from the numerical solutions in Figs. 5(d)–5(f). Figure 7 shows a good comparison between the exponent calculated from the numerical solutions from the AME and the one calculated from Monte Carlo simulations. The dependence of $\gamma(z, T)$ with the parameters z and T is qualitatively similar to the dependence of $\alpha(z, T)$.

IV. DYNAMICS ON A MOORE LATTICE

The Threshold model in a two-dimensional regular lattice with a Moore neighborhood (nearest and next-nearest neighbors) is known to have a critical threshold (cascade condition) $T_c = 3/8$ [22]. Below this value, the cascade dynamics follows a power-law increase in the density of adopters, $\rho(t) \sim t^2$, which does not depend on the threshold value T. In Fig. 8(a), we show a typical realization of this model: From an initial seed, the adoption radius increases linearly with time until all agents adopt the technology.

When aging is considered, the cascade dynamics become much slower and a dependence on T appears. When the aging mechanism is exogenous, Monte Carlo simulations indicate cascade dynamics following a power law $\rho(t) \approx t^{\zeta(T)}$. Qualitatively, we observe that while in the case without aging there was a soft interface between adopter and nonadopters, aging causes a strong roughening in the interface and the presence of nonadopters inside the bulk [see Fig. 8(b)]. In addition, the exponent values fitted from Monte Carlo simulations allow us to collapse curves for different system sizes [see Fig. 9(a)]. Due to finite-size effects, the interface between adopters and nonadopters eventually reaches the borders of the system and the remaining nonadopters, in the bulk will slowly adopt with the density of adopters following the functional shape $\rho(t) = 1 - 1/(t + 2)$.

Figure 8(c) shows the dynamics towards global adoption for endogenous aging. In comparison with the case of exogenous aging, we do not observe strong interface roughening between adopters and nonadopters because nonadopters are not present in the bulk. Monte Carlo simulations indicate a very slow increase of the density of adopters ρ, similar to a
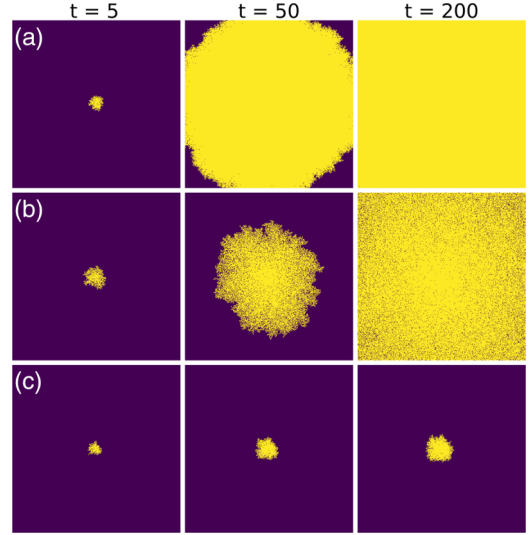

FIG. 8. Cascade spreading of (a) the original Threshold model and the versions with (b) exogenous and (c) endogenous aging on a Moore neighborhood lattice with size $N = L \times L$, $L = 405$. Yellow and purple nodes are adopters and nonadopters, respectively. Time increases from left to right. Initial seeds are selected favoring cascades: one agent and all his or her neighbors are set as adopters at the center of the system.
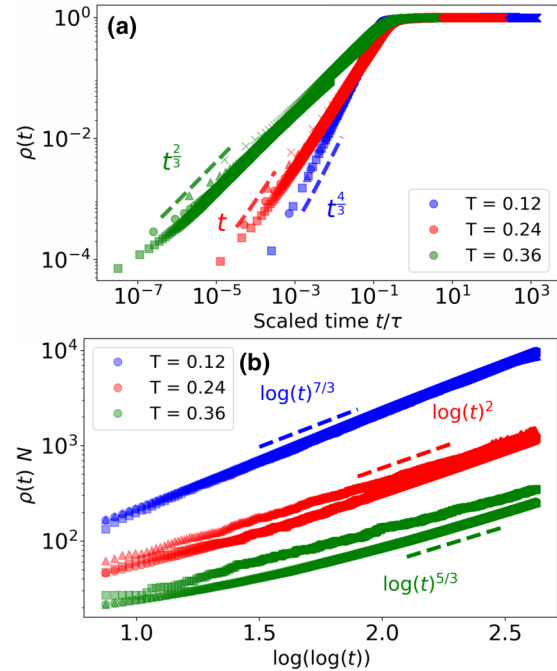

FIG. 9. Cascade dynamics of the Threshold model with (a) exogenous and (b) endogenous aging on a Moore neighborhood lattice. Different colors indicate different values of the threshold T. Different markers indicate the results of Monte Carlo simulations with different system size $N = L \times L$: $L = 50$ (crosses), 100 (triangles), 200 (circles), and 400 (squares). In (a), time is scaled according to size $\tau = L^{2/\zeta}$. Discontinuous solid lines indicate a power-law behavior with exponent $\zeta = 4/3$ (blue), 1 (red), and 2/3 (green). In (b), the system sizes are not scaled due to the slow dynamics. Discontinuous solid lines indicate a power-logarithmic behavior, $\rho(t)N \sim \ln(t)^\nu$, with exponent $\nu = 7/3$ (blue), 2 (red), and 5/3 (green).

power-logarithmic growth $\rho(t) \approx [\ln(t)]^\nu$, with a threshold-dependent exponent $\nu(T)$ [Fig. 9(b)]. Unfortunately, we were not able to find an analytical framework for the Threshold model in a Moore lattice. Our general approximation used for complex networks assumes a treelike network and is not appropriate for this case.

V. CONCLUSIONS

We have addressed, in this work, the role of aging in general models with binary-state agents interacting in a complex network. Temporal activity patterns are incorporated by means of a variable that represents the internal time of each agent. We have developed an approximate master equation for this general situation. In this framework, we have explicitly studied the effect of aging in the Threshold model as a paradigmatic example of complex contagion processes. Aging implies a lower probability to change the state when the internal time increases. We considered two aging mechanisms: endogenous aging, in which the internal time measures the persistence time in the current state, and exogenous aging, in which the internal time measures the time since the last update attempt.

Our theoretical framework with some approximations to attain analytical results provides a good description of the results from Monte Carlo simulations for Erdős-Rényi, random-regular, and Barabási-Albert networks. For these three types of complex networks, we found that the cascade condition T_c (critical value of the threshold parameter T as a function of mean degree z of the network) for the full spreading from an initial seed is not changed by the aging mechanisms. However, aging modifies, in nontrivial ways, the cascade dynamics of the process. The exponential growth with exponent $\alpha(z, T)$ of the density of adopters in the absence of aging becomes a power law with exponent $\delta(z, T)$ for endogenous aging, and a stretched exponential characterized by an exponent $\gamma(z, T)$ for exogenous aging. We have analyzed the exponents' dependence with the order parameters $\alpha(z, T)$, $\delta(z, T)$, and $\gamma(z, T)$, and shown that $\delta(z, T) = \alpha(z, T)$.

Our general theoretical framework, based on the assumption of a treelike network, is not appropriate for a regular lattice. In this case, we have only been able to run Monte Carlo simulations. Our results indicate that exogenous aging gives rise to adoption dynamics characterized by an increase in the interface roughness, by the presence of nonadopters in the bulk, and by a power-law growth of the density of adopters with exponent $\zeta(T)$, while in the absence of aging, $\zeta = 2$ independently of T. Endogenous aging, on the other hand, produces very slow (logarithmiclike) dynamics, with a threshold-dependent exponent $\nu(T)$.

This work highlights the importance of non-Markovian dynamics in general binary-state dynamics and, specifically, in the Threshold model. For the problem of innovation adoption that this model addresses, we show how persistence times have an important impact on the adoption cascade. In fact, in the lattice, for $T = 2/8$ and exogenous aging, we recover a linear evolution for the number of adopters as in Ref. [62] for a mean-field model. Further work in this direction would be to categorize technologies according to the adoption curve, to show if the system has important resistance to the pre-
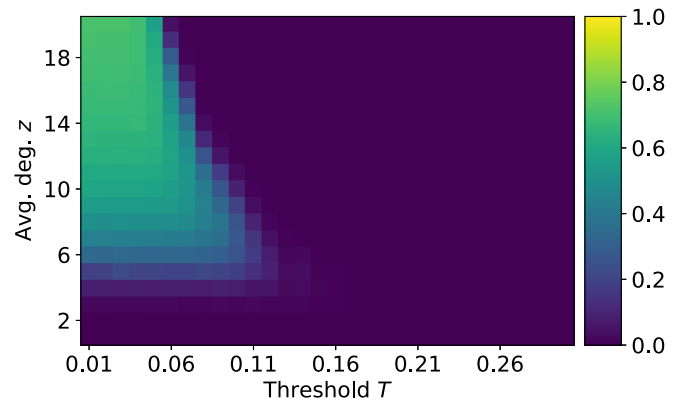

FIG. 10. Average density ρ of adopters for an Erdős-Rényi graph of mean degree z using the symmetrical Threshold model with endogenous aging with threshold T. The activation probability is exponential, $p_A(j) = \exp[-0.5 * (j + 1)]$. Color-coded values of ρ are from Monte Carlo simulations of the model without aging in a graph with $N = 10\,000$ agents. Monte Carlo simulations are averaged over $M = 5 \times 10^4$ realizations.

vious technology (endogenous aging), or a balance between memory and external influence or advertisement (exogenous aging). Furthermore, the theoretical framework presented here gives a basis for further investigations of the memory effects and non-Markovian dynamics in networks, and in particular for binary-state models with aging. Still, a number of theoretical developments remain open for future work, such as the consideration of stochastic finite-size effects [74]. Also, proper approximations need to be developed to account for some of our numerical results for random-regular networks with high degree, as well as for high clustering, degree-degree correlations networks and for regular lattices, including continuous field equations for this latter case.

APPENDIX A: ACTIVATION PROBABILITY EFFECT ON THE CASCADE CONDITION

For our chosen activation probability $p_A = 1/(j + 2)$, it has been shown that aging is not able to modify the cascade condition from the original Threshold model. It is natural to ask about the generality of this result. In fact, in Fig. 10 we show that for an exponential activation probability ($p_A = \exp[-0.5(j + 1)]$), the cascade condition is modified and the system does not reach the absorbing state for any values of the average degree z and the threshold T considered before (compare with Fig. 1).

One may think that this different behavior is because not all nodes are able to activate and adopt the technology with the exponential activation function. To clarify this issue, we computed the probability that an agent never activates during the whole evolution. Since we are performing a random asynchronous update in a network of size N, the probability P that an agent is not activated in an update attempt is the probability of not being chosen plus the probability of being chosen and not activating:

$$P\,[\text{``agent is not activated in an attempt''}]$$

$$= \left(1 - \frac{1}{N}\right) + \frac{1}{N}(1 - p_A(j)). \tag{A1}$$

As we are performing Monte-Carlo simulations, the probability P of the agent being not activated after the N update attempts of the Monte-Carlo step is:

$$P\,[\text{``agent is not activated in a MC step''}]$$

$$= \left[\left(1 - \frac{1}{N}\right) + \frac{1}{N}(1 - p_A(j))\right]^N. \tag{A2}$$

Therefore, the probability P that an agent is never activated is the probability that the agent does not get activated during the evolution, in other words, after infinite Monte-Carlo steps (where after each Monte-Carlo, since it has not been activated, the internal time j increases by one):

$$P\,[\text{``agent is never activated''}]$$

$$= \prod_{j=0}^{\infty} \left[\left(1 - \frac{1}{N}\right) + \frac{1}{N}(1 - p_A(j))\right]^N. \tag{A3}$$

For both activation probabilities, exponential ($p_A(j) = \exp(-0.5(j+1))$) and power law ($p_A(j) = 1/(j+2)$), following Eq. (A3), the probability that an agent is never activated tends to 0 for the long time simulation limit $j_{\max} \to \infty$ for any system size N. Therefore, all agents in the system activate at least once during the simulation. Thus, the reason that an exponential activation probability is able to change the cascade condition and a power law function is not just an activation effect, it is due to a non-trivial balance between activation and the adoption process. Notice that this calculation is the same for both aging mechanisms (endogenous and exogenous) because the difference between those appears after the first activation.

APPENDIX B: DERIVATION OF A GENERAL MASTER EQUATION FOR BINARY-STATE MODELS WITH AGING IN COMPLEX NETWORKS

We consider binary-state dynamics on static, undirected, connected networks assuming a locally treelike structure and in the limit of $N \to \infty$, closely following the approach used in Ref. [64] for binary-state dynamics in complex networks. The relevant ingredient is to consider the nodes with different age as different sets, what allows us to treat as Markovian the memory effects introduced by aging [19,48]. We define $s_{k,m,j}(t)$ [$i_{k,m,j}(t)$] as the fraction of nodes that are susceptible [infected] and have degree k, m infected neighbors and age j at time t. The networks have degree distribution p_k and have
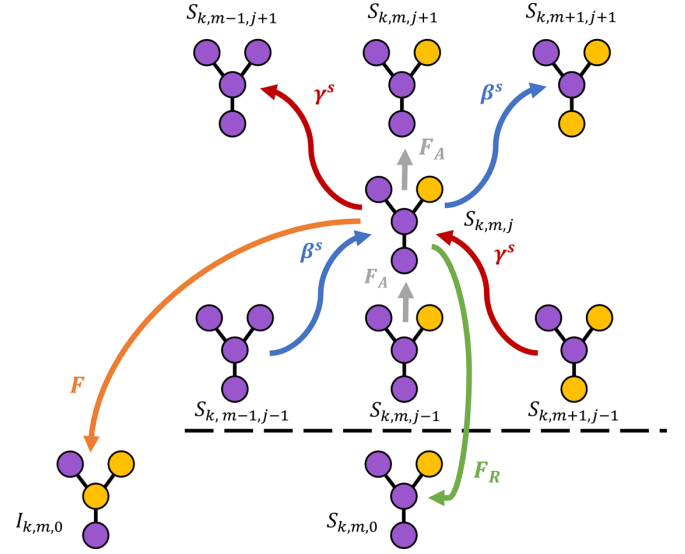

FIG. 11. Schematic representation of the transitions to or from the set $s_{k,m,j}$ ($j > 0$). We show the central node with some neighbors for different values m and j. Purple nodes are susceptible, non-adopters, or spin down, and yellow are infected, adopters, or spin up.

been generated by the configuration model [69,70]. The initial condition is set such that all agents have age $j = 0$ and there is a randomly chosen fraction ρ_0 of nodes that are infected,

$$\text{For } j > 0, \quad s_{k,m,j}(0) = 0, \quad i_{k,m,j}(0) = 0;$$
$$\text{For } j = 0, \quad s_{k,m,0}(0) = (1 - \rho_0)\,B_{k,m}[\rho_0],$$
$$i_{k,m,0}(0) = \rho_0\,B_{k,m}[\rho_0], \tag{B1}$$

where $B_{k,m}[\rho_0]$ is the binomial distribution with k attempts, m successes, and ρ_0 is the initial fraction of infected agents that is the probability of success of the binomial. Now, we examine how $s_{k,m,j}$ changes in a time step. We separately consider the case $j = 0$ since its evolution is different from $j > 0$. See Fig. 11 for a schematic representation of transitions involving $s_{k,m,j}$.

This is the way to reach the expressions of Eq. (B2):

$$s_{k,m,j}(t + dt) = s_{k,m,j}(t) - F(k, m, j)\,s_{k,m,j}\,dt$$
$$- F_R(k, m, j)\,s_{k,m,j}\,dt - F_A(k, m, j)\,s_{k,m,j}\,dt$$
$$+ F_A(k, m, j - 1)\,s_{k,m,j-1}\,dt$$
$$- \omega(s_{k,m,j} \to s_{k,m+1,j+1})\,s_{k,m,j}\,dt$$
$$- \omega(s_{k,m,j} \to s_{k,m-1,j+1})\,s_{k,m,j}\,dt$$
$$+ \omega(s_{k,m+1,j-1} \to s_{k,m,j})\,s_{k,m+1,j-1}\,dt$$
$$+ \omega(s_{k,m-1,j-1} \to s_{k,m,j})\,s_{k,m-1,j-1}\,dt,$$

$$s_{k,m,0}(t + dt) = s_{k,m,0}(t) - F(k, m, 0)\,s_{k,m,0}\,dt$$
$$+ \sum_{l=0}^{\infty} R(k, m, l)\,i_{k,m,l}\,dt$$
$$+ \sum_{l=1}^{\infty} F_R(k, m, l)\,s_{k,m,l}\,dt$$

$$- F_A(k, m, 0) \, s_{k,m,0} \, dt$$
$$- \omega(s_{k,m,0} \to s_{k,m+1,1}) \, s_{k,m,0} \, dt$$
$$- \omega(s_{k,m,0} \to s_{k,m-1,1}) \, s_{k,m,0} \, dt. \tag{B2}$$

Similar equations can be found considering transitions for $i_{k,m,j}$. In these equations, the transition probabilities (described in detail in Sec. III B) allow agents to change their state (F and R), reset their internal time ($j \to 0$) (F_R and R_R and age ($j \to j + 1$) (F_A and R_A). Notice that we have considered no transition increasing (or decreasing) the number of infected neighbors, m, keeping constant the age j. This is because the age j is defined as the time spent in the current state (or since a reset). Therefore, if a node remains susceptible and the number of infected neighbors changes ($m \to m \pm 1$), the age of the node must increase ($j \to j + 1$). To determine the rate of these events, we use the same assumption as in Ref. [64]: we assume that the number of S-S edges (edges between susceptible agents) change to S-I edges (edges between susceptible and infected agents) at a time-dependent rate β^s. Therefore, the transition rates are

$$\omega(s_{k,m,j} \to s_{k,m+1,j+1}) = (k - m) \, \beta^s,$$
$$\omega(s_{k,m-1,j-1} \to s_{k,m,j}) = (k - m + 1) \, \beta^s. \tag{B3}$$

To determine the rate β^s, we count the change of S-S edges that change to S-I in a time step. This change is produced by a neighbor changing state from susceptible to infected. Thus, we can extract this information from the infection probability $F(k, m, j)$,

$$\beta^s = \frac{\sum_{j=0}^{\infty} \sum_{k=0}^{\infty} p_k \sum_{m=0}^{k} (k - m) \, F(k, m, j) \, s_{k,m,j}}{\sum_{j=0}^{\infty} \sum_{k=0}^{\infty} p_k \sum_{m=0}^{k} (k - m) \, s_{k,m,j}}. \tag{B4}$$

A similar approximation is used to determine the transition rates at which S-I edges change to S-S edges. We write

$$\omega(s_{k,m,j} \to s_{k,m-1,j+1}) = m \, \gamma^s,$$
$$\omega(s_{k,m+1,j-1} \to s_{k,m,j}) = (m + 1) \, \gamma^s, \tag{B5}$$

where the rate γ^s is computed using the recovery probability $R(k, m, j)$,

$$\gamma^s = \frac{\sum_{j=0}^{\infty} \sum_{k=0}^{\infty} p_k \sum_{m=0}^{k} (k - m) \, R(k, m, j) \, i_{k,m,j}}{\sum_{j=0}^{\infty} \sum_{k=0}^{\infty} p_k \sum_{m=0}^{k} (k - m) \, i_{k,m,j}}. \tag{B6}$$

For standard models, one natural assumption is to consider the probability to age as the probability of neither changing state nor resetting,

$$F(k, m, j) + F_A(k, m, j) + F_R(k, m, j) = 1,$$
$$R(k, m, j) + R_A(k, m, j) + R_R(k, m, j) = 1. \tag{B7}$$

With this condition, taking the limit $dt \to 0$ of Eq. (B2), we obtain the approximate master equation (AME) for

the evolution of the different sets $s_{k,m,j}$, $s_{k,m,0}$ $i_{k,m,j}$, and $i_{k,m,0}$:

$$\frac{ds_{k,m,j}}{dt} = - s_{k,m,j} - (k - m) \, \beta^s \, s_{k,m,j} - m \, \gamma^s \, s_{k,m,j}$$
$$+ (k - m + 1) \, \beta^s \, s_{k,m-1,j-1}$$
$$+ (m + 1) \, \gamma^s \, s_{k,m+1,j-1}$$
$$+ F_A(k, m, j - 1) \, s_{k,m,j-1},$$

$$\frac{ds_{k,m,0}}{dt} = - s_{k,m,0} - (k - m) \, \beta^s \, s_{k,m,0} - m \, \gamma^s \, s_{k,m,0}$$
$$+ \sum_{l=0}^{\infty} R(k, m, l) \, i_{k,m,l} + \sum_{l=0}^{\infty} F_R(k, m, l) \, s_{k,m,l},$$

$$\frac{di_{k,m,j}}{dt} = - i_{k,m,j} - (k - m) \, \beta^i \, i_{k,m,j} - m \, \gamma^i \, i_{k,m,j}$$
$$+ (k - m + 1) \, \beta^i \, i_{k,m-1,j-1} + (m + 1) \, \gamma^i \, i_{k,m+1,j-1}$$
$$+ R_A(k, m, j - 1) \, i_{k,m,j-1},$$

$$\frac{di_{k,m,0}}{dt} = - i_{k,m,0} - (k - m) \, \beta^i \, i_{k,m,0} - m \, \gamma^i \, i_{k,m,0}$$
$$+ \sum_{l=0}^{\infty} F(k, m, l) \, s_{k,m,l} + \sum_{l=0}^{\infty} R_R(k, m, l) \, i_{k,m,l},$$
$$\tag{B8}$$

where β^i and γ^i are similar rates as β^s [Eq. (B4)] and γ^s [Eq. (B6)], exchanging terms $s_{k,m,j}$ by $i_{k,m,j}$ and vice versa. These equations define a closed set of deterministic differential equations that can be solved numerically using standard computational methods for any complex network and any model aging via the infection and recovery, reset, and aging probabilities (a general script in JULIA is available in the author's GitHub repository [75]).

The model is introduced via the transition probabilities (F, R, F_A, R_A, F_R, R_R), which may depend on the degree k, the number of infected neighbors, m, and the time spent in the actual state (or since a reset) j. For the Threshold model with aging, dynamics are monotonic and there are no age dynamics once the agent is infected, $R(k, m, j) = R_A(k, m, j) = R_R(k, m, j) = 0$. Therefore, the equations for $s_{k,m,0}$ decouple from the equations for the variables $i_{k,m,j}$, reducing Eq. (B8) to

$$\frac{ds_{k,m,j}}{dt} = - s_{k,m,j} - (k - m) \, \beta^s \, s_{k,m,j}$$
$$+ (k - m + 1) \, \beta^s \, s_{k,m-1,j-1}$$
$$+ F_A(k, m, j - 1) \, s_{k,m,j-1},$$

$$\frac{ds_{k,m,0}}{dt} = - s_{k,m,0} - (k - m) \, \beta^s \, s_{k,m,0}$$
$$+ \sum_{l=0}^{\infty} F_R(k, m, l) \, s_{k,m,l}. \tag{B9}$$

[1] T. M. Liggett *et al.*, *Stochastic Interacting Systems: Contact, Voter and Exclusion Processes* (Springer Science & Business Media, New York, 1999), Vol. 324.

[2] V. Sood and S. Redner, Voter Model on Heterogeneous Graphs, Phys. Rev. Lett. **94**, 178701 (2005).

[3] J. Fernández-Gracia, K. Suchecki, J. J. Ramasco, M. San Miguel, and V. M. Eguíluz, Is the Voter Model a Model for Voters?, Phys. Rev. Lett. **112**, 158701 (2014).

[4] S. Redner, Reality-inspired Voter models: A mini-review, C. R. Phys. **20**, 275 (2019).

[5] M. Granovetter, Threshold models of collective behavior, Am. J. Sociol. **83**, 1420 (1978).

[6] R. Pastor-Satorras, C. Castellano, P. Van Mieghem, and A. Vespignani, Epidemic processes in complex networks, Rev. Mod. Phys. **87**, 925 (2015).

[7] M. Diakonova, M. San Miguel, and V. M. Eguíluz, Absorbing and shattered fragmentation transitions in multilayer coevolution, Phys. Rev. E **89**, 062818 (2014).

[8] M. Diakonova, V. Nicosia, V. Latora, and M. San Miguel, Irreducibility of multilayer network dynamics: The case of the Voter model, New J. Phys. **18**, 023010 (2016).

[9] R. Amato, N. E. Kouvaris, M. San Miguel, and A. Díaz-Guilera, Opinion competition dynamics on multiplex networks, New J. Phys. **19**, 123019 (2017).

[10] F. Vazquez, V. M. Eguíluz, and M. S. Miguel, Generic Absorbing Transition in Coevolution Dynamics, Phys. Rev. Lett. **100**, 108702 (2008).

[11] G. F. de Arruda, G. Petri, and Y. Moreno, Social contagion models on hypergraphs, Phys. Rev. Res. **2**, 023032 (2020).

[12] I. Iacopini, G. Petri, A. Barrat, and V. Latora, Simplicial models of social contagion, Nat. Commun. **10**, 2485 (2019).

[13] G. Cencetti, F. Battiston, B. Lepri, and M. Karsai, Temporal properties of higher-order interactions in social networks, Sci. Rep. **11**, 7028 (2021).

[14] C. Castellano, M. A. Muñoz, and R. Pastor-Satorras, Nonlinear q-Voter model, Phys. Rev. E **80**, 041129 (2009).

[15] A. F. Peralta, A. Carro, M. San Miguel, and R. Toral, Analytical and numerical study of the non-linear noisy Voter model on complex networks, Chaos: Interdis. J. Nonlinear Sci. **28**, 075516 (2018).

[16] A. Carro, R. Toral, and M. San Miguel, The noisy Voter model on complex networks, Sci. Rep. **6**, 24775 (2016).

[17] P. Van Mieghem and R. van de Bovenkamp, Non-Markovian Infection Spread Dramatically Alters the Susceptible-Infected-Susceptible Epidemic Threshold in Networks, Phys. Rev. Lett. **110**, 108701 (2013).

[18] M. Starnini, J. P. Gleeson, and M. Boguñá, Equivalence between Non-Markovian and Markovian Dynamics in Epidemic Spreading Processes, Phys. Rev. Lett. **118**, 128301 (2017).

[19] A. F. Peralta, N. Khalil, and R. Toral, Reduction from non-Markovian to Markovian dynamics: The case of aging in the noisy-Voter model, J. Stat. Mech. (2020) 024004.

[20] H. Chen, S. Wang, C. Shen, H. Zhang, and G. Bianconi, Non-Markovian majority-vote model, Phys. Rev. E **102**, 062311 (2020).

[21] D. J. Watts, A simple model of global cascades on random networks, Proc. Natl. Acad. Sci. USA **99**, 5766 (2002).

[22] D. Centola, V. M. Eguíluz, and M. W. Macy, Cascade dynamics of complex propagation, Phys. A **374**, 449 (2007).

[23] Damon Centola, *How Behavior Spreads: The Science of Complex Contagions* (Princeton University Press, Princeton, NJ, 2018), p. 308; Science **361**, 1320 (2018).

[24] J. P. Gleeson and D. J. Cahalane, Seed size strongly affects cascades on random networks, Phys. Rev. E **75**, 056103 (2007).

[25] J. P. Gleeson, Cascades on correlated and modular random networks, Phys. Rev. E **77**, 046117 (2008).

[26] A. Hackett, S. Melnik, and J. P. Gleeson, Cascades on a class of clustered random networks, Phys. Rev. E **83**, 056107 (2011).

[27] A. Hackett and J. P. Gleeson, Cascades on clique-based graphs, Phys. Rev. E **87**, 062801 (2013).

[28] F. Diaz-Diaz, M. San Miguel, and S. Meloni, Echo chambers and information transmission biases in homophilic and heterophilic networks, Sci. Rep. **12**, 9350 (2022).

[29] Q.-H. Liu, F.-M. Lü, Q. Zhang, M. Tang, and T. Zhou, Impacts of opinion leaders on social contagions, Chaos: Interdis. J. Nonlinear Sci. **28**, 053103 (2018).

[30] P. Singh, S. Sreenivasan, B. K. Szymanski, and G. Korniss, Threshold-limited spreading in social networks with multiple initiators, Sci. Rep. **3**, 2330 (2013).

[31] P. S. Dodds, K. D. Harris, and C. M. Danforth, Limited Imitation Contagion on Random Networks: Chaos, Universality, and Unpredictability, Phys. Rev. Lett. **110**, 158701 (2013).

[32] A. Czaplicka, R. Toral, and M. San Miguel, Competition of simple and complex adoption on interdependent networks, Phys. Rev. E **94**, 062301 (2016).

[33] B. Min and M. San Miguel, Competing contagion processes: Complex Contagion triggered by Simple Contagion, Sci. Rep. **8**, 10422 (2018).

[34] D. Centola, The spread of behavior in an online social network experiment, Science **329**, 1194 (2010).

[35] F. Karimi and P. Holme, Threshold model of cascades in empirical temporal networks, Phys. A **392**, 3476 (2013).

[36] M. Karsai, G. Iñiguez, K. Kaski, and J. Kertész, Complex Contagion process in spreading of online innovation, J. R. Soc. Interface **11**, 20140694 (2014).

[37] S. B. Rosenthal, C. R. Twomey, A. T. Hartnett, H. S. Wu, and I. D. Couzin, Revealing the hidden networks of interaction in mobile animal groups allows prediction of complex behavioral contagion, Proc. Natl. Acad. Sci. USA **112**, 4690 (2015).

[38] M. Karsai, G. Iñiguez, R. Kikas, K. Kaski, and J. Kertész, Local cascades induced global contagion: How heterogeneous thresholds, exogenous effects, and unconcerned behaviour govern online adoption spreading, Sci. Rep. **6**, 27178 (2016).

[39] B. Mønsted, P. Sapieżyński, E. Ferrara, and S. Lehmann, Evidence of Complex Contagion of information in social media: An experiment using Twitter bots, PLoS ONE **12**, e0184148 (2017).

[40] S. Unicomb, G. Iñiguez, and M. Karsai, Threshold driven contagion on weighted networks, Sci. Rep. **8**, 3094 (2018).

[41] D. Guilbeault and D. Centola, Topological measures for identifying and predicting the spread of Complex Contagions, Nat. Commun. **12**, 4430 (2021).

[42] J. L. Iribarren and E. Moro, Impact of Human Activity Patterns on the Dynamics of Information Diffusion, Phys. Rev. Lett. **103**, 038702 (2009).

[43] M. Karsai, M. Kivelä, R. K. Pan, K. Kaski, J. Kertész, A.-L. Barabási, and J. Saramäki, Small but slow world: How network topology and burstiness slow down spreading, Phys. Rev. E **83**, 025102(R) (2011).

[44] D. Rybski, S. V. Buldyrev, S. Havlin, F. Liljeros, and H. A. Makse, Communication activity in a social network: Relation between long-term correlations and inter-event clustering, Sci. Rep. **2**, 560 (2012).

[45] M. Zignani, A. Esfandyari, S. Gaito, and G. P. Rossi, Walls-in-one: Usage and temporal patterns in a social media aggregator, Appl. Network Sci. **1**, 5 (2016).

[46] O. Artime, J. J. Ramasco, and M. San Miguel, Dynamics on networks: Competition of temporal and topological correlations, Sci. Rep. **7**, 41627 (2017).

[47] P. Kumar, E. Korkolis, R. Benzi, D. Denisov, A. Niemeijer, P. Schall, F. Toschi, and J. Trampert, On interevent time distributions of avalanche dynamics, Sci. Rep. **10**, 626 (2020).

[48] A. F. Peralta, N. Khalil, and R. Toral, Ordering dynamics in the Voter model with aging, Phys. A **552**, 122475 (2020).

[49] P. S. Dodds and D. J. Watts, Universal Behavior in a Generalized Model of Contagion, Phys. Rev. Lett. **92**, 218701 (2004).

[50] M. Shrestha and C. Moore, Message-passing approach for threshold models of behavior in networks, Phys. Rev. E **89**, 022805 (2014).

[51] J. P. Gleeson, K. P. O'Sullivan, R. A. Baños, and Y. Moreno, Effects of Network Structure, Competition and Memory Time on Social Spreading Phenomena, Phys. Rev. X **6**, 021019 (2016).

[52] S.-W. Oh and M. A. Porter, Complex Contagions with timers, Chaos: Interdis. J. Nonlinear Sci. **28**, 033101 (2018).

[53] H.-U. Stark, C. J. Tessone, and F. Schweitzer, Decelerating Microdynamics Can Accelerate Macrodynamics in the Voter Model, Phys. Rev. Lett. **101**, 018701 (2008).

[54] J. Fernández-Gracia, V. M. Eguíluz, and M. San Miguel, Update rules and interevent time distributions: Slow ordering versus no ordering in the Voter model, Phys. Rev. E **84**, 015103(R) (2011).

[55] T. Pérez, K. Klemm, and V. M. Eguíluz, Competition in the presence of aging: Dominance, coexistence, and alternation between states, Sci. Rep. **6**, 21128 (2016).

[56] M. Boguñá, L. F. Lafuerza, R. Toral, and M. A. Serrano, Simulating non-Markovian stochastic processes, Phys. Rev. E **90**, 042108 (2014).

[57] O. Artime, A. F. Peralta, R. Toral, J. J. Ramasco, and M. San Miguel, Aging-induced continuous phase transition, Phys. Rev. E **98**, 032104 (2018).

[58] D. Abella, M. San Miguel, and J. J. Ramasco, Aging effects in Schelling segregation model, Sci. Rep. **12**, 19376 (2022).

[59] E. M. Rogers, A. Singhal, and M. M. Quinlan, Diffusion of innovations, in *An Integrated Approach to Communication Theory and Research* (Routledge, 2014), p. 432.

[60] F. M. Bass, A new product growth for model consumer durables, Manag. Sci. **15**, 215 (1969).

[61] S. Galam, Sociophysics: A review of Galam models, Intl. J. Mod. Phys. C **19**, 409 (2008).

[62] S. Gonalves, M. F. Laguna, and J. R. Iglesias, Why, when, and how fast innovations are adopted, Eur. Phys. J. B **85**, 192 (2012).

[63] J. P. Gleeson, High-Accuracy Approximation of Binary-State Dynamics on Networks, Phys. Rev. Lett. **107**, 068701 (2011).

[64] J. P. Gleeson, Binary-State Dynamics on Complex Networks: Pair Approximation and Beyond, Phys. Rev. X **3**, 021004 (2013).

[65] J. Fernández-Gracia, V. M. Eguíluz, and M. San Miguel, Timing Interactions in Social simulations: The Voter Model, arXiv:1306.4735v1.

[66] N. C. Wormald *et al.*, Models of random regular graphs, London Math. Soc. Lecture Note Ser., 239 (1999).

[67] P. Erdős, A. Rényi *et al.*, On the evolution of random graphs, Publ. Math. Inst. Hung. Acad. Sci. **5**, 17 (1960).

[68] A.-L. Barabási, Scale-free networks: A decade and beyond, Science **325**, 412 (2009).

[69] M. Molloy and B. Reed, A critical point for random graphs with a given degree sequence, Random Struct. Algorithms **6**, 161 (1995).

[70] M. E. J. Newman, S. H. Strogatz, and D. J. Watts, Random graphs with arbitrary degree distributions and their applications, Phys. Rev. E **64**, 026118 (2001).

[71] Here we use the term "master equation" for consistency with Refs. [63,64], but the word "master" has a different meaning than the one used to describe an equation for the probability distribution [74].

[72] N. C. Wormald, Models of random regular graphs, in *Surveys in Combinatorics, 1999*, edited by J. D. Lamb and D. A. Preece, London Mathematical Society Lecture Note Series (Cambridge University Press, Cambridge, 1999), pp. 239–298.

[73] L. A. Keating, J. P. Gleeson, and D. J. P. O'Sullivan, Multitype branching process method for modeling Complex Contagion on clustered networks, Phys. Rev. E **105**, 034306 (2022).

[74] A. F. Peralta and R. Toral, Binary-state dynamics on complex networks: Stochastic pair approximation and beyond, Phys. Rev. Res. **2**, 043370 (2020).

[75] Github repository, https://github.com/davidabbu/Aging-in-binary-state-models.